



HAL
open science

C1-Linked Spirobifluorene Dimers Pure Hydrocarbon Hosts for High-Performance Blue Phosphorescent OLEDs

Lambert J Sicard, Hong-Cheng Li, Qiang Wang, Xiang-Yang Liu, Olivier Jeannin, Joëlle Rault-Berthelot, Liang-Sheng Liao, Zuo-Quan Jiang, Cyril Poriel

► **To cite this version:**

Lambert J Sicard, Hong-Cheng Li, Qiang Wang, Xiang-Yang Liu, Olivier Jeannin, et al.. C1-Linked Spirobifluorene Dimers Pure Hydrocarbon Hosts for High-Performance Blue Phosphorescent OLEDs. *Angewandte Chemie International Edition*, 2019, 58 (12), pp.3848-3853. 10.1002/anie.201813604 . hal-02050274

HAL Id: hal-02050274

<https://univ-rennes.hal.science/hal-02050274>

Submitted on 22 Mar 2019

HAL is a multi-disciplinary open access archive for the deposit and dissemination of scientific research documents, whether they are published or not. The documents may come from teaching and research institutions in France or abroad, or from public or private research centers.

L'archive ouverte pluridisciplinaire **HAL**, est destinée au dépôt et à la diffusion de documents scientifiques de niveau recherche, publiés ou non, émanant des établissements d'enseignement et de recherche français ou étrangers, des laboratoires publics ou privés.

C1-Linked Spirobifluorene Dimers: Pure Hydrocarbon Hosts for High Performance Blue Phosphorescent OLEDs

Lambert Sicard, Hong-Cheng Li, Qiang Wang, Xiang-Yang Liu, Olivier Jeannin, Joëlle Rault-Berthelot, Liang-Sheng Liao, Zuo-Quan Jiang,* Cyril Poriel*

Abstract: We report C1-linked spirobifluorene dimers. A comprehensive study is carried out to analyse the electronic properties of these highly twisted structures. This work shows the C1 position enables the design of high triplet pure hydrocarbon materials for hosting blue phosphors in efficient Phosphorescent OLEDs (PhOLEDs). As far as we know, this work displays the highest performance blue PhOLEDs ever reported for pure hydrocarbons (external quantum efficiency of ~23%), highlighting the potential of the C1-spirobifluorene scaffold in organic electronics.

Since their discovery,^[1] Phosphorescent Organic Light-Emitting Diodes (PhOLEDs), which use heavy-metal complexes emitters dispersed in a host material have attracted great attention.^[1-4] In such devices, it is crucial to prevent energy back transfers from the emitter to the host and to favour the confinement of excitons. This can be achieved by combining in the host a high triplet energy (E_T) and a balanced hole/electron transport. The classic molecular design strategy consists in linking, within the host, an electron-rich fragment with an electron-poor fragment and to induce a π -conjugation disruption between them. This allows to adjust the molecular frontier orbitals energy levels without extending the conjugation length, keeping a high E_T . Various electron-rich (carbazole,^[5, 6] quinolinophenothiazine,^[7] dihydroacridine^[8] etc) and electron-poor (phosphine oxide,^[6] pyridine,^[9, 10] dimesitylboron^[8] etc) building units have been used to construct highly efficient bipolar host materials for PhOLEDs. However, functional groups possessing heteroatoms lead to important stability issues, which hinder the technological development of PhOLEDs. In operating devices, it has been demonstrated that C-S, C-P, or C-N bonds are significantly weaker than a C-C bond, which lead to a strong decrease of the device stability.^[11] As the stability of organic devices is one of the most important features to address for the future of organic electronics, the quest for highly efficient hosts exclusively built from pure hydrocarbon (PHC) backbones could potentially offer a good option.^[10] However, PHC hosts very rarely lead to high performance PhOLEDs and still lag far behind hosts containing heteroatoms. For example, in the field of blue emitting PhOLEDs, which is the most challenging nowadays, the results based on PHC hosts are still low with external quantum efficiencies (EQEs) of ca. 10/12%,^[2, 10, 12-15] and only one example of an EQE above 20% reported to date.^[16] On the other hand, many hosts incorporating heteroatoms can lead to EQEs above 20%.^[8, 17, 18] Designing efficient PHC hosts for high-triplet blue phosphors is hence the final obstacle in the development of PhOLEDs. In this work, we report a new molecular design strategy towards very high efficiency PHC hosts, namely Spirobifluorene (SBF) dimers linked from C1: **1,1''-(SBF)₂**, **1,2''-(SBF)₂**, **1,3''-(SBF)₂** and **1,4''-(SBF)₂**, Chart 1. We notably

show that the nature of the bridged biphenyl linkages (*ortho*, *meta* and *para*) and the dihedral angle between the connected fluorenes both have remarkable and different consequences on the electronic properties (E_T , HOMO/LUMO energies, charge transport). Thanks to the C1-SBF scaffold, all four dimers enable high performance blue PhOLEDs when incorporated as hosts. The better hole/electron balance of the C1/C3 linked dimer **1,3''-(SBF)₂** compared to its regioisomers leads to an external quantum efficiency (EQE) of ~23%, the highest reported to date for PHC. As C1-SBFs are almost absent from literature, this work demonstrates the potential of this scaffold and open new avenues in the field of PHC for organic electronics.

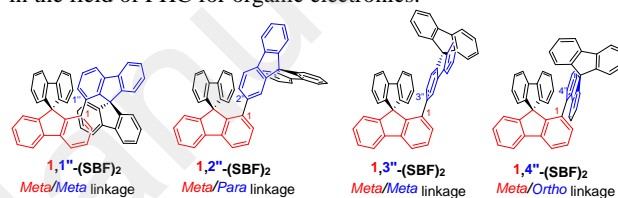
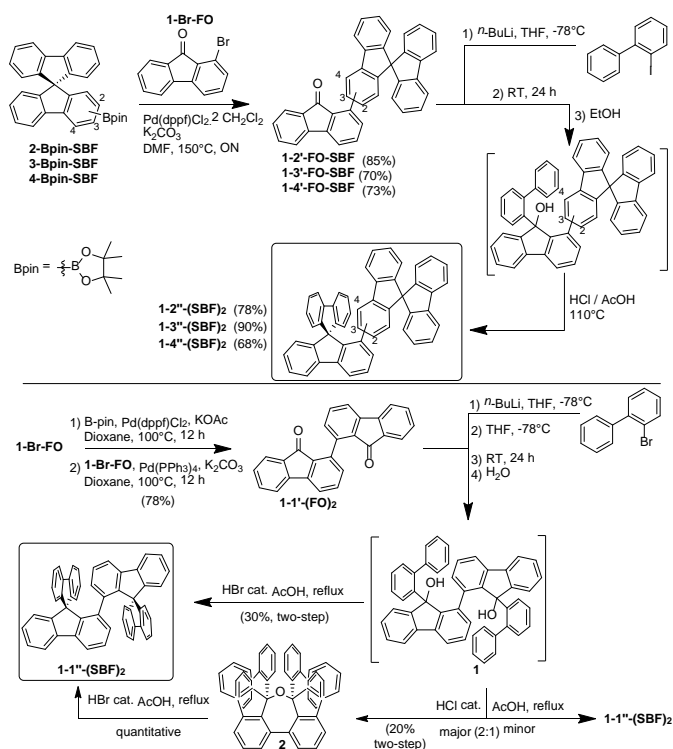


Chart 1. SBF dimers: **1,1''-(SBF)₂**, **1,2''-(SBF)₂**, **1,3''-(SBF)₂** and **1,4''-(SBF)₂**.

In materials science, chemists aim to synthesize target organic-semiconductors in a short and efficient manner and if possible by using common synthetic intermediates (Scheme 1). **1,2''-(SBF)₂**, **1,3''-(SBF)₂** and **1,4''-(SBF)₂** were synthesized following a similar approach starting from their corresponding pinacol derivatives, **2-Pin-SBF**, **3-Pin-SBF** and **4-Pin-SBF**. First, couplings with 1-bromofluorenone **1-Br-FO**^[19] were performed providing the corresponding fluorenones **1,2'-FO-SBF**, **1,3'-FO-SBF** and **1,4'-FO-SBF** with a pending SBF unit. Note that the yields of the coupling reactions at C1 of fluorenones are high (70 to 85%, Scheme 1-top) and weakly dependent of the SBF substitution pattern. The lithium-bromine exchange of 2-iodobiphenyl followed by the addition of fluorenones afforded the corresponding fluorenols, which were further involved in an electrophilic intramolecular aromatic substitution to provide the dimers **1,2''-(SBF)₂**, **1,3''-(SBF)₂** and **1,4''-(SBF)₂** with high yields. It is interesting to note that despite a sterically hindered environment, the spirolinked fluorenes can be efficiently introduced in the last step with the pending SBF already in place. However, due to this steric congestion, **1,1''-(SBF)₂** had to be synthesized following a different strategy (Scheme 1-bottom). Thus, **1-Br-FO** was first dimerized through a one-pot Pd-catalysed coupling to give the ketone dimer **1,1'-(FO)₂** before forming the bis-diol intermediate **1** following the strategy described above. But interestingly, we found that the ether derivative **2** was the main product of the intramolecular dehydration with the HCl/AcOH catalysed cyclization (**2** and **1,1''-(SBF)₂** are formed in a 2:1 ratio). Fortunately, compound **2** could be cleaved by HBr and the resulting tertiary bromide spontaneously transferred to the target *spiro* compound **1,1''-(SBF)₂** in high yield. The final cyclisation step of **1** was hence optimized using the HBr/AcOH medium directly (30% yield). To conclude, the four C1-linked dimers have been synthesized at the gram scale by short and efficient paths.

[*]L. J. Sicard, Dr C. Poriel, Dr J. Rault-Berthelot, Dr O. Jeannin- Univ Rennes, CNRS, ISCR- UMR 6226, F-35000 Rennes, France. cyril.poriel@univ-rennes1.fr
H.-C. Li, Q. Wang, X. Y. Liu, Prof. Z.-Q. Jiang, Prof. L.-S. Liao, Institute of Functional Nano & Soft Materials, Soochow University, Suzhou 215123, P.R. China. zqjiang@suda.edu.cn. L. J. Sicard and H.-C. Li contributed equally to this work.

[**]We thank the ANR (CE05-0024), the NSFC (51873139 & 21572152), the NANO-CIC, the PAPD, the 111 Project, the CDIFX and CRMPO, the CINES (2018-A0040805032) Dr C. Quinton for help in modelling and Drs B. Donnio and B. Heinrich for TGA.



Scheme 1. Syntheses of the four SBF dimers.

The structural arrangement of the four dimers obtained from X-Ray diffraction of single crystals is depicted in Figure 1-right. In addition to the nature of the linkage (*ortho*, *meta* and *para*) between two chromophores, the dihedral angle between them is of chief importance in regard to the electronic coupling/decoupling.^[20] The most relevant structural feature is therefore the relative position of the two substituted fluorene backbones, which drive most of the electronic properties described below. The dihedral angle between the mean plane of the two substituted phenyl rings of the fluorenes increases as follows: 54.9° for **1,2''-(SBF)₂**, 57.9° for **1,3''-(SBF)₂**, 61.1° for **1,1''-(SBF)₂** and 76.9° for **1,4''-(SBF)₂**. The torsion angle recorded for **1,2''-(SBF)₂** is impressively larger than those usually reported for a non-encumbered phenyl/fluorene *para* linkage.^[20] This structural feature is of key importance since a *para* linkage usually maximises the conjugation between two fragments.^[20] We will see later that the strong steric hindrance imposed by the SBF substituted at C1 induces a π -conjugation disruption. In **1,3''-(SBF)₂**, the *meta* linkage leads to a similar angle between the two fluorenyl fragments, 57.9°. This angle is also higher than those usually found for 3-substituted SBFs.^[16, 20] The case of **1,1''-(SBF)₂** is more surprising since its dihedral angle (61.1°), despite the strong steric congestion imposed by the two linked C1 positions (shown below by ¹H NMR) is decreased compared to a SBF substituted at C1 by a simple phenyl ring (75.4°).^[20] Therefore, it seems the torsion angle is lowered in order to minimize the π - π interactions between the two sets of cofacial fluorenes. Thus, the two hydrogen atoms in α position of the dimer linkage present very short CH- π distances, 2.76/2.78 Å, with the centroid of their respective facing phenyl rings (Figure 1 and S1). Furthermore, these hydrogen atoms are subjected, in ¹H NMR, to the shielding anisotropy cones of the phenyl rings, displaying a dramatically upfield shifted signal at 5.65 ppm. The presence of five unusually broad signals corresponding to the H2, H3 and H4 protons of the unsubstituted fluorenes also translates the strong sterically hindered environment of **1,1''-(SBF)₂** (See

NMR variable temperature studies in Figures S22-23). Thus, **1,1''-(SBF)₂** displays a singular molecular arrangement compared to the other dimers, which must be at the origin of its specific electronic properties described below. In **1,4''-(SBF)₂**, the presence of one SBF in *ortho* position of the other leads to an impressive enhancement of the dihedral angle, recorded at 76.9°. This structural feature is assigned to a combination of the steric congestions imposed by (i) the *ortho* proton facing the pendant phenyl in C4 and (ii) the unsubstituted fluorene opposite to the C4 substituted fluorene.^[10, 13] As far as we know, this dihedral angle is one of the highest reported for C4-substituted SBFs.^[10] Due to the sterically hindered environment observed in the four molecular structures, many short C/C and C/H distances (shorter than the sum of their Van der Waals radii) are measured (see Tables S1-S4). Thus, in the four dimers, the relative position of the SBF fragments provides different molecular arrangements with specific steric hindrances. This feature will be one of the key parameters involved in the electronic properties described below.

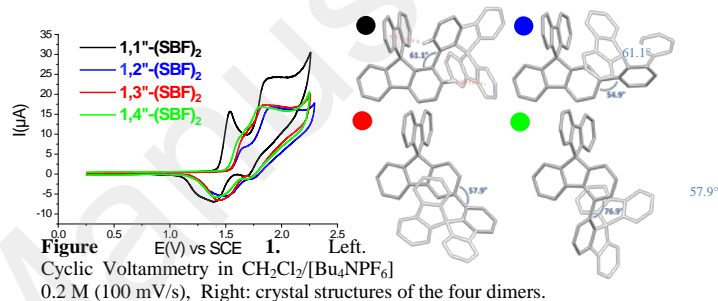


Figure 1. Cyclic Voltammograms (CV) of **1,2''-(SBF)₂**, **1,3''-(SBF)₂** and **1,4''-(SBF)₂** in CH_2Cl_2 [Bu_4NPF_6] 0.2 M (100 mV/s), Right: crystal structures of the four dimers.

Table 1. Properties and device performance of SBF dimers and SBF.

	1,1''-(SBF)₂	1,2''-(SBF)₂	1,3''-(SBF)₂	1,4''-(SBF)₂	SBF^[13, 20]	
λ_{ABS} (eV) ^a [nm] ($\times 10^4 \text{ L mol}^{-1} \text{ cm}^{-1}$)	300 (0.86)	297 (2.23)	298.5 (0.84)	297.5 (2.00)	297 (0.72)	
	312 (1.23)	309.5 (2.67)	316 (1.31)	309.5 (3.07)	308 (1.45)	
			(sh, 1.54)			
λ_{EM}^b (nm)	325	334	320	326	310, 323	
QY	0.32	0.79	0.59	0.45	0.40	
τ_f [ns]	4.6	2.0	4.4	4.2	4.6	
k_r ($\times 10^7$) [s^{-1}]	7.0	39	13	11	8.7	
k_{nr} ($\times 10^7$) [s^{-1}]	15	10	9.3	13	13	
τ_p [s]	5.2	4.9	5.5	5.5	5.3	
LUMO (eV)	Exp ^b	-1.84	-2.11	-2.01	-1.90	-1.74
	Calc ^d	-1.37	-1.38	-1.35	-1.37	-1.26
HOMO (eV)	Exp ^b	-5.84	-5.95	-5.95	-5.92	-5.95
	Calc ^d	-5.86	-5.87	-5.89	-5.87	-5.99
ΔE (eV)	Opt ^e	3.88	3.83	3.94	3.92	3.97
	Exp ^b	4.00	3.84	3.94	4.02	4.21
	Calc ^d	4.49	4.49	4.54	4.50	4.73
E_T (eV)	Opt ^e	2.85	2.80	2.87	2.86	2.88
	Calc ^f	2.63	2.55	2.67	2.64	2.86
Thermal (°C)	T_g	145	143	147	145	-
	T_d	339	310	330	324	234
EQE (%)		20.1	20.3	22.9	19.1	6.6
		40.3	38.5	45.5	38.5	20.6
CE (Cd/A)	32.9	34.5	36.3	32.7	-	
PE (Lm/W)	2.9	2.7	2.9	2.9	3.3	

a. in cyclohexane, b. from CVs, c. from UV-Vis spectra, d. from DFT calculations, e. in 2-Me-THF, f. from TD-DFT calculations

The cyclic voltammograms (CV, Figure 1, left) of **1,2''-(SBF)₂**, **1,3''-(SBF)₂** and **1,4''-(SBF)₂** are similar, with a first

mono-electronic wave (detected as a shoulder at 1.6 V) followed by a multi-electronic wave at potentials over 1.8 V. The HOMO energies were evaluated at -5.95, -5.95 and -5.92 eV for **1,2''-(SBF)₂**, **1,3''-(SBF)₂** and **1,4''-(SBF)₂** respectively, Table 1. Thus, despite their different substitution patterns, **1,2''-(SBF)₂**, **1,3''-(SBF)₂** and **1,4''-(SBF)₂** interestingly display very comparable HOMO energy levels, similar to that of the building block **SBF** (-5.95 eV). This can be understood by the electronic distribution of their HOMO, which presents density only on one SBF (Figure 2-middle). Thus, due to the large dihedral angle between two connected fluorenes, their electronic coupling seems fully broken. The CV of **1,1''-(SBF)₂** is surprisingly different, displaying a first wave shifted to a lower potential (1.53 V). In addition, this wave is bielectronic whereas the first wave of the other isomers was found to be mono-electronic. These features clearly show that the fluorene units are in a different environment than that above exposed. The HOMO of **1** (-5.84 eV) is therefore the highest of the series despite sharing a similar strong steric hindrance with its isomers. As exposed above, the 1,1'' connection leads to a particular arrangement of **1,1''-(SBF)₂** with sp^2 -CH- π interactions and π - π interactions between facing fluorenes which must induce this peculiar CV. Due to the symmetry of the molecule, one can indeed consider that the two cofacial fluorene dimers are concomitantly oxidized. This is supported by the delocalization of the HOMO, which is spread out on the entire molecule and not only on one SBF as mentioned above for the three other isomers. The cathodic explorations reveal a different behaviour. Indeed, the LUMO energy of **1,2''-(SBF)₂** is the lowest of the series (-2.11 eV), indicating a certain degree of coupling between the two connected fluorenes (unlike the HOMO). Thus, for **1,2''-(SBF)₂**, the torsion (steric effect) between the two fluorenes seems to have a significantly greater impact on the HOMO energy than on the LUMO energy (that shows influence of the electronic effect of the *para* linkage). The electronic delocalization of the LUMO, which is spread out on the two sigma-linked fluorenes (Figure 2-top) clearly shows this feature. Thus, the dihedral angle has a different influence on the benzenoidal HOMO/quinooidal LUMO distribution, providing an interesting way to selectively tune their energies. The same effect is observed for **1,3''-(SBF)₂** (LUMO = -2.01 eV) but is less pronounced. There is hence a different impact of the linkage and its torsion on the HOMO/LUMO distribution. Again, the LUMO of **1,1''-(SBF)₂** (-1.84 eV) does not follow this trend as it is spread out on the four fluorenes due to symmetry considerations.

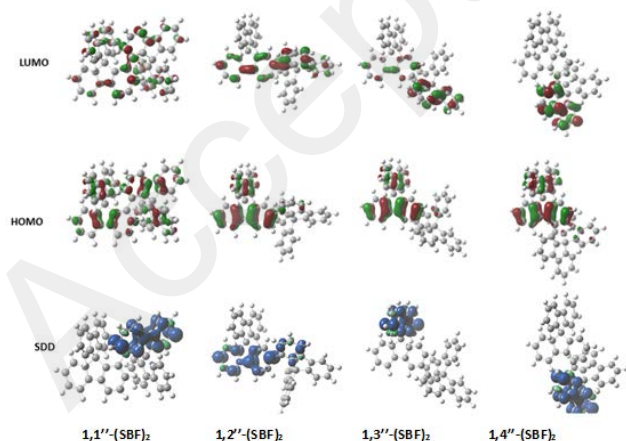


Figure 2. Frontier molecular orbitals and triplet spin density of the SBF dimers

The UV-Vis absorption spectra of the dimers display the same overall structure with nevertheless striking differences (Figure 3-left). They all present two characteristic bands at 297-300 and 308-312 nm (in addition to the phenyl characteristic bands below 280 nm), which are also found in the **SBF** building block (Table

1).^[13] **1,2''-(SBF)₂** displays the most singular spectrum with an additional and large band at 316 nm. This band (assigned from TD-DFT mainly to a HOMO→LUMO transition), possessing a high oscillator strength ($f = 0.25$, see Figure S18), reflects a certain degree of conjugation between the two connected fluorenes and a good overlap between the orbitals. As exposed above, this extension of conjugation is enabled by the *para* linkage of the C2-substituted SBF, which leads to a fluorene/fluorene electronic coupling despite the high dihedral angle between them. The absorption spectra of the three other dimers show no trace of such a low energy band (assigned by TD-DFT to an almost forbidden HOMO-LUMO transition with a very weak oscillator strength, see Figure S17, S19 and S20) but reveal a main band at 309.5 nm (for **1,3''-(SBF)₂** and **1,4''-(SBF)₂**) assigned to various transitions involving HOMO-1/LUMO and/or HOMO/LUMO-1 contributions. These absorption spectra are also almost identical with that of their **SBF** building block, showing that the π -conjugation between the two **SBF** units is largely broken. However, a striking difference for **1,1''-(SBF)₂** is observed: its main band displays a 4 nm bathochromic shift in respect to its dimer isomers and **SBF**. We assign this feature to the strong tilt undergone by the unsubstituted fluorenes (to minimize interaction with their cofacial substituted fluorenes) of **1,1''-(SBF)₂** (see Figure S1), that alters the spiroconjugation. In fluorescence (Figure 3-right), the same trend as that exposed above is observed for the four dimers. Indeed, **1,1''-(SBF)₂**, **1,3''-(SBF)₂** and **1,4''-(SBF)₂** possess an almost identical emission spectrum both in shape and wavelengths, with maxima comprised between 320 and 325 nm. **1,2''-(SBF)₂** displays the most red-shifted spectrum (334 nm) due to its extended conjugation. Such a structureless emission is rare for SBF derivatives and assigned to the congestion imposed to the sigma link hindering the planarization at the excited state, hence inducing a greater number of emitting conformers. The four spectra remain in the near UV region (despite the connection of two fluorenes) which is a key point for their use as hosts in PhOLEDs.

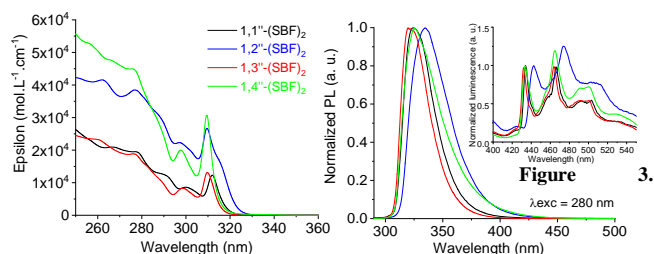


Figure 3. Absorption (left) and Emission (right) at rt in cyclohexane; Inset: Emission at 77 K in 2-Me-THF of the SBF dimers

Thus, from a spectral shape point of view, **1,1''-(SBF)₂**, **1,3''-(SBF)₂** and **1,4''-(SBF)₂** are difficult to discriminate despite the different nature of the linkages. Analyses of time resolved fluorescence data provide important information on their activation/deactivation processes. Indeed, the compounds display different quantum yields (QY), ie 0.32 for **1,1''-(SBF)₂**, 0.59 for **1,3''-(SBF)₂** and 0.45 for **1,4''-(SBF)₂** but almost identical fluorescence lifetimes (4.6, 4.4 and 4.2 ns respectively, Table 1). The radiative rate constant (k_r) of **1,1''-(SBF)₂** is calculated to be $7.0 \times 10^7 \text{ s}^{-1}$ and at the origin of the QY loss compared to **1,3''-(SBF)₂** ($k_r = 13 \times 10^7 \text{ s}^{-1}$) and **1,4''-(SBF)₂** ($k_r = 11 \times 10^7 \text{ s}^{-1}$). Oppositely, the k_r value calculated for **1,2''-(SBF)₂** is much higher, $39 \times 10^7 \text{ s}^{-1}$, indicating a stronger electronic transition moment, which is at the origin of its superior QY (0.79). The presence of an additional SBF unit in the structure of the dimers would, in principle, allow additional non-radiative pathways of the excited states deactivation processes compared to its monomer **SBF**. However, the non-radiative rate constant (k_{nr}) remains remarkably almost unchanged for the four dimers,

indicating similar vibrational deactivation pathways despite their different structural environments. Thus, except the k_r (and resulting QY) of **1,2''-(SBF)₂**, the radiative/non-radiative constants and QY of all the dimers are very similar to those of **SBF**, translating the fact that the dimers behave as an isolated SBF unit in the deactivation of their excited states. At 77 K, the emission spectra of the four dimers present a well resolved phosphorescence contribution with long lifetimes comprised between 4.9 and 5.5 s, Table 1. Their intensities can be correlated to the fluorescence QY: the higher the QY, the less intense the phosphorescence contribution. This translates a more or less efficient intersystem crossing between S_1 and T_1 . The corresponding E_T of **1,1''-(SBF)₂**, **1,2''-(SBF)₂**, **1,3''-(SBF)₂** and **1,4''-(SBF)₂** were evaluated at 2.85, 2.80, 2.87 and 2.86 eV (Figure 3-right, inset). The E_T of **1,1''-(SBF)₂**, **1,3''-(SBF)₂** and **1,4''-(SBF)₂** are very high and close to that of **SBF** ($E_T = 2.88$ eV) as the triplet exciton is efficiently confined on one fluorene (Figure 2, bottom). As it is known that spiroconjugation decreases E_T from fluorene to **SBF**,^[20] the slightly lowered value for **1,1''-(SBF)₂** could again be assigned to the tilt of its unsubstituted fluorenes, altering the spiroconjugation (see Figure S1 for structural details). This is in accordance with the conclusion drawn from the UV-vis absorption spectra. Oppositely, the triplet exciton of **1,2''-(SBF)₂** is spread out on two fluorenes, which decreases the E_T to 2.80 eV, a value nevertheless high for a 2-substituted SBF.^[10] Thus, the E_T of the four dimers are high enough to prevent reverse energy transfers from the bis(3,5-difluoro-2-(2-pyridyl)phenyl-(2-carboxypyridyl)iridium(III) (FIrpic) blue phosphor ($E_T = 2.64$ eV) to the host in the triplet manifold, making them eligible as hosts in blue PhOLEDs. In summary, the nature of the linkages and the dihedral angle between the fluorenes have different impacts on the singlet, triplet and HOMO/LUMO energies allowing some degree of tunability.

In order to confirm the efficiency of the design for electronic applications, the dimers were studied by thermogravimetric analyses (TGA) and differential scanning calorimetry (DSC), see Figure S13 and S14. Due to the presence of the two rigid spiro bridges, all four dimers present high thermal stability with a 5% mass loss occurring between 310 and 339 °C. In addition, high glass transitions T_g (comprised between 143 and 147 °C, Table 1) are also measured by DSC with no detection of other phase transitions (melting, crystallization). Thus, the thermal and morphological characteristics of the four dimers are much improved over their constituting building block **SBF** which presents a lower T_d of 234 °C and a crystallisation transition at 135 °C.^[13] Thus, the dimers maintain some excellent properties of **SBF** (such as its E_T) while enhancing others (such as the T_g/T_d). This is in fact the strength of the present dimer design.

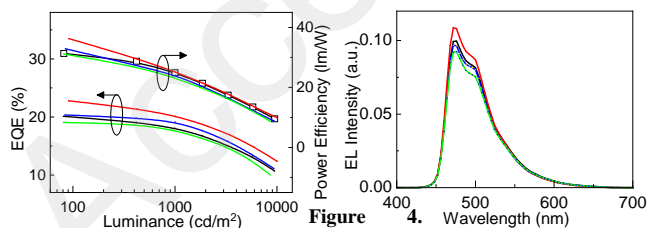


Figure 4. External Quantum Efficiency and Power Efficiency vs Luminance (Left) and Electroluminescence spectra (right) of SBF dimers based PhOLEDs

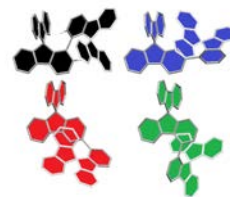
In order to finally explore the potential of these C1-linked SBF dimers for organic electronics, they were incorporated as hosts in blue PhOLED doped with FIrpic. The device configuration and the energy level scheme are presented in the SI (Figure S16). The key data are summarized in Table 1. As shown in Figure 4-right, all the devices exhibited identical blue emission peaked at 472 nm and same Commission Internationale de

L'Eclairage coordinates of (0.14, 0.35), showing an excellent energy transfer cascade. The EQE_{max} were all very high, 20.1%, 20.3%, 22.9% and 19.1% for **1,1''-(SBF)₂**, **1,2''-(SBF)₂**, **1,3''-(SBF)₂** and **1,4''-(SBF)₂** respectively, Figure 4-left. The current (power) efficiencies of all the devices were also high ranging from 38.5 Cd/A (32.7 Lm/W) for **1,4''-(SBF)₂** to 45.5 Cd/A (36.3 Lm/W) for **1,3''-(SBF)₂**. There is no doubt that the C1-SBF scaffold is at the origin of these performances. The turn-on voltages (V_{on}) of all the devices were found to be below 3V, a low value for blue emission translating an excellent charge injection in such PHC systems. It should be noted that the device using **1,2''-(SBF)₂** displays a slightly lower V_{on} (2.7 V) compared to the others (2.9 V), which is consistent with its narrowest energy gap. The highest EQE, 22.9%, was achieved by **1,3''-(SBF)₂**, which is as far as we are aware, the highest value for a PHC host reported to date in literature. To better understand this high performance, charges transport properties of the four dimers were further measured by the space charge limited current (SCLC) model (Figure S15, Table S6), which can be assigned to the second region in the J-V curves of the charge only devices under low bias. We found that **1,3''-(SBF)₂** possesses the most favourable carrier mobilities of the series. In hole-only and electron-only measurements, **1,3''-(SBF)₂** indeed presents a hole mobility of $1.35 \times 10^{-6} \text{ cm}^2 \text{ V}^{-1} \text{ s}^{-1}$, and the highest electron mobility of $4.09 \times 10^{-8} \text{ cm}^2 \text{ V}^{-1} \text{ s}^{-1}$ in the series.

To conclude, this work reports the first examples of C1-linked SBF dimers as PHC materials for electronics. The substitution at C1 has many advantages such as keeping a high E_T , and inducing excellent thermal properties while providing some degree of tunability of other properties (charge transport). The role played by the substitution pattern on the electronic properties has been particularly highlighted. Incorporation of the dimers as hosts in blue PhOLEDs has led to very high-performance devices with low V_{on} and the highest EQE reported to date for PHC in the case of **1,3''-(SBF)₂**. With such high performance, PHC semiconductors can undoubtedly play a role in the future of organic electronics.

- [1]M. A. Baldo, D. F. O'Brien, Y. You, A. Shoustikov, S. Sibley, M. E. Thompson, S. R. Forrest, *Nature* **1998**, *395*, 151-154.
 [2]Y. Tao, C. Yang, J. Qin, *Chem. Soc. Rev.* **2011**, *40*, 2943-2970.
 [3]L. Xiao, Z. Chen, B. Qu, J. Luo, S. Kong, Q. Gong, J. Kido, *Adv. Mater.* **2011**, *23*, 926-952.
 [4]H. Sasabe, J. Kido, *Eur. J. Org. Chem.* **2013**, 1653-1663.
 [5]C. Quinton, S. Thiery, O. Jeannin, D. Tondelier, B. Geffroy, E. Jacques, J. Rault-Berthelot, C. Poriel, *ACS Appl. Mater. Interfaces* **2017**, *9*, 6194-6206.
 [6]A. Maheshwaran, V. G. Sree, H.-Y. Park, H. Kim, S. H. Han, J. Y. Lee, S.-H. Jin, *Adv. Funct. Mater.* **2018**, *28*, 1802945-1802951.
 [7]C. Poriel, J. Rault-Berthelot, S. Thiery, C. Quinton, O. Jeannin, U. Biapo, B. Geffroy, D. Tondelier, *Chem. Eur. J.* **2016**, *22*, 17930-17935.
 [8]M.-M. Xue, C.-C. Huang, Y. Yuan, L.-S. Cui, Y.-X. Li, B. Wang, Z.-Q. Jiang, M.-K. Fung, L.-S. Liao, *ACS Appl. Mater. Interfaces* **2016**, *8*, 20230-20236.
 [9]Q. Bai, H. Liu, L. Yao, T. Shan, J. Li, Y. Gao, Z. Zhang, Y. Liu, P. Lu, B. Yang, Y. Ma, *ACS Appl. Mater. Interfaces* **2016**, *8*, 24793-24802.
 [10]C. Poriel, J. Rault-Berthelot, *J. Mater. Chem. C* **2017**, *5*, 3869-3897
 [11]N. Lin, J. Qiao, L. Duan, L. Wang, Y. Qiu, *J. Phys. Chem. C* **2014**, *118*, 7569-7578.
 [12]M. Romain, S. Thiery, A. Shirinskaya, C. Declairieux, D. Tondelier, B. Geffroy, O. Jeannin, J. Rault-Berthelot, R. Métivier, C. Poriel, *Angew. Chem. Int. Ed.* **2015**, *54*, 1176-1180.
 [13]S. Thiery, D. Tondelier, C. Declairieux, G. Seo, B. Geffroy, O. Jeannin, J. Rault-Berthelot, R. Métivier, C. Poriel, *J. Mater. Chem. C* **2014**, *2*, 4156-4166.
 [14]C. Fan, Y. Chen, P. Gan, C. Yang, C. Zhong, J. Qin, D. Ma, *Org. Lett.* **2010**, *12*, 5648-5651.
 [15]M. Zhuo, W. Sun, G. Liu, J. Wang, L. Guo, C. Liu, B. Mi, J. Song, Z. Gao, *J. Mater. Chem. C* **2015**, *3*, 9137-9144.
 [16]L.-S. Cui, Y.-M. Xie, Y.-K. Wang, C. Zhong, Y.-L. Deng, X.-Y. Liu, Z.-Q. Jiang, L.-S. Liao, *Adv. Mater.* **2015**, *27*, 4213-4217.

- [17]C.-C. Lai, M.-J. Huang, H.-H. Chou, C.-Y. Liao, P. Rajamalli, C.-H. Cheng, *Adv. Funct. Mat.* **2015**, *25*, 5548-5556.
- [18]X. Li, J. Zhang, Z. Zhao, L. Wang, H. Yang, Q. Chang, N. Jiang, Z. Liu, Z. Bian, W. Liu, Z. Lu, C. Huang, *Adv. Mater.* **2018**, *30*, 1705005.
- [19]X.-Y. Chen, S. Ozturk, E. J. Sorensen, *Org. Lett.* **2017**, *19*, 1140-1143.
- [20]L. Sicard, C. Quinton, J.-D. Peltier, D. Tondelier, B. Geffroy, U. Biapo, R. Métivier, O. Jeannin, J. Rault-Berthelot, C. Poriel, *Chem. Eur. J.* **2017**, *23*, 7719-7723.



Pure Hydrocarbon Semi-conductors

Lambert Sicard, Hong-Cheng Li, Qiang Wang, Xiang-Yang Liu, Olivier Jeannin, Joëlle Rault-Berthelot, Liang-Sheng Liao, Zuo-Quan Jiang,* Cyril Poriel*

C1-Linked Spirobifluorene Dimers: Pure Hydrocarbon Hosts for High Performance Blue Phosphorescent OLEDs

We report highly twisted C1-linked spirobifluorene dimers linked from the C1 position. This work shows the C1 position enables the design of high triplet pure hydrocarbon materials for hosting blue phosphors in highly efficient Phosphorescent OLEDs (PhOLEDs).

